Characterisation of seismic activity at a kimberlite block caving operation in a complex geological setting in Quebec, Canada

RL Westley-Hauta *Stornoway Diamonds, Canada*

S Meyer *Institute of Mine Seismology, Canada*

Abstract

Stornoway Diamonds' Renard Mine is an inclined block caving operation that began underground production of more than 6,000 tonnes per day from two kimberlite pipes in 2018. After the resumption of operations in September 2020 after a temporary shutdown due to the COVID-19 pandemic, it was observed by underground workers and the mine's ground control department that the seismic activity rate had increased. Three large events greater than magnitude MN 2 occurred within one month during the spring of 2021. Based on underground observations, the probable source of these events was a normal fault slip in proximity to a 90,000 m³ underground void, and no major damage to active excavations was observed.

A seismic system was brought online in September 2021, and it has served numerous functions to date, most important of which is to enhance the understanding the seismic hazard in the mine's active excavations. A considerable portion of the seismic activity has taken place between the primary Renard 2 pipe (R2) and the nearby smaller secondary Renard 3 pipe (R3) located 100 m to the southeast of the R2 pipe which indicates a strong interaction between these zones. Moment tensor inversions were completed of more than 1,000 seismic events; the mine's in situ stress orientation was estimated and used to calibrate the mine's numerical models. The source mechanisms of the seismic events are contextualised with spatial data related to mining activities to categorise the seismicity (such as caving events and slip-type events on geological structures) and to understand the rock mass response to mining over time. The seismic system is used by the mining operation to visualise the seismicity in real time, and in collaboration with the Institute of Mine Seismology, analysis of the seismic data has allowed the operation to understand the seismic response to mining in a complex geological setting.

Keywords: *block caving, seismicity, moment tensor inversion, kimberlite, stress*

1 Introduction

Stornoway Diamonds' Renard Mine is an inclined block caving operation located in the Otish mountains of Quebec more than 800 km north of the city of Montreal, Canada. Commercial surface operations began in January 2017, and underground production started in 2018. The 'Renard Cluster' consists of nine kimberlite pipes as shown in Figure 1.

These kimberlite pipes are classified as diatreme-zone kimberlites consisting of multiple pyroclastic units surrounded by granitoid and gneissic host rock which are intersected and altered by numerous dykes and irregular intrusive geological structures.

In 2022, underground production at a rate of more than 6,000 tonnes per day took place primarily in the mid-sized R2 pipe and a smaller irregular pipe R3 located ~100 m to the southeast of R2. The underground workings consist of three lifts with the third lift scheduled to begin production in the second quarter of 2022. Two views of the underground mine workings and open pit are shown in Figure 2.
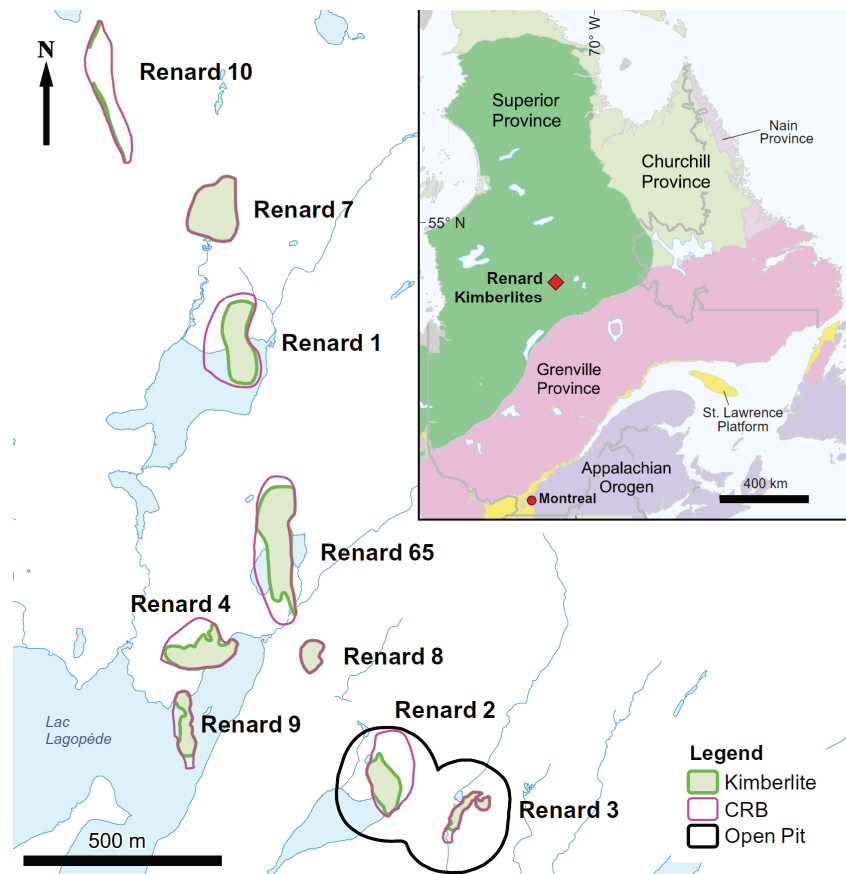
Characterisation of seismic activity at a kimberlite block caving operation in a complex geological setting in Quebec, Canada

RL Westley-Hauta & S Meyer

Figure 1 Location of the Renard kimberlite cluster comprised of nine pipes which are outlined in pink (Lépine & Farrow 2018)
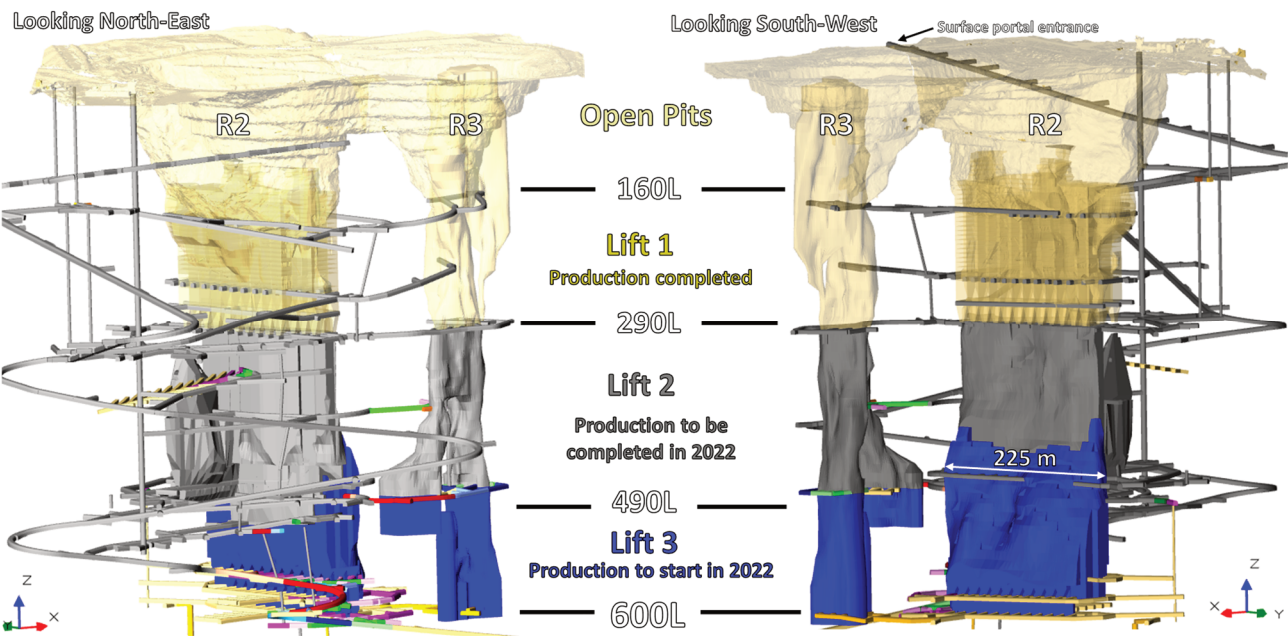

Figure 2 Views of the open pit and underground workings for Renard Mine; elevations are shown in units of m below surface

All ore is hauled via the mine's main ramp to the surface stockpiles where the ore is then fed into the onsite mill.

1.1   Mining method

Once underground production had begun in 2018 in the mid-sized R2 pipe using a blasthole shrinkage stope (BHS) mining method, it was realised that the rock mass caved more easily than expected, and the mining method was modified to an inclined block cave type method. The inclined block cave layout consists of groups of three levels per lift.

Drawpoints are 5.3 m wide and the distance between the centre of the drawpoints is 15 m to achieve interaction between the 'draw ellipsoids'. An illustrative plan and section view of Lift 3 is shown in Figures 3 and 4 which illustrates the planned draw columns that will interact during extraction.
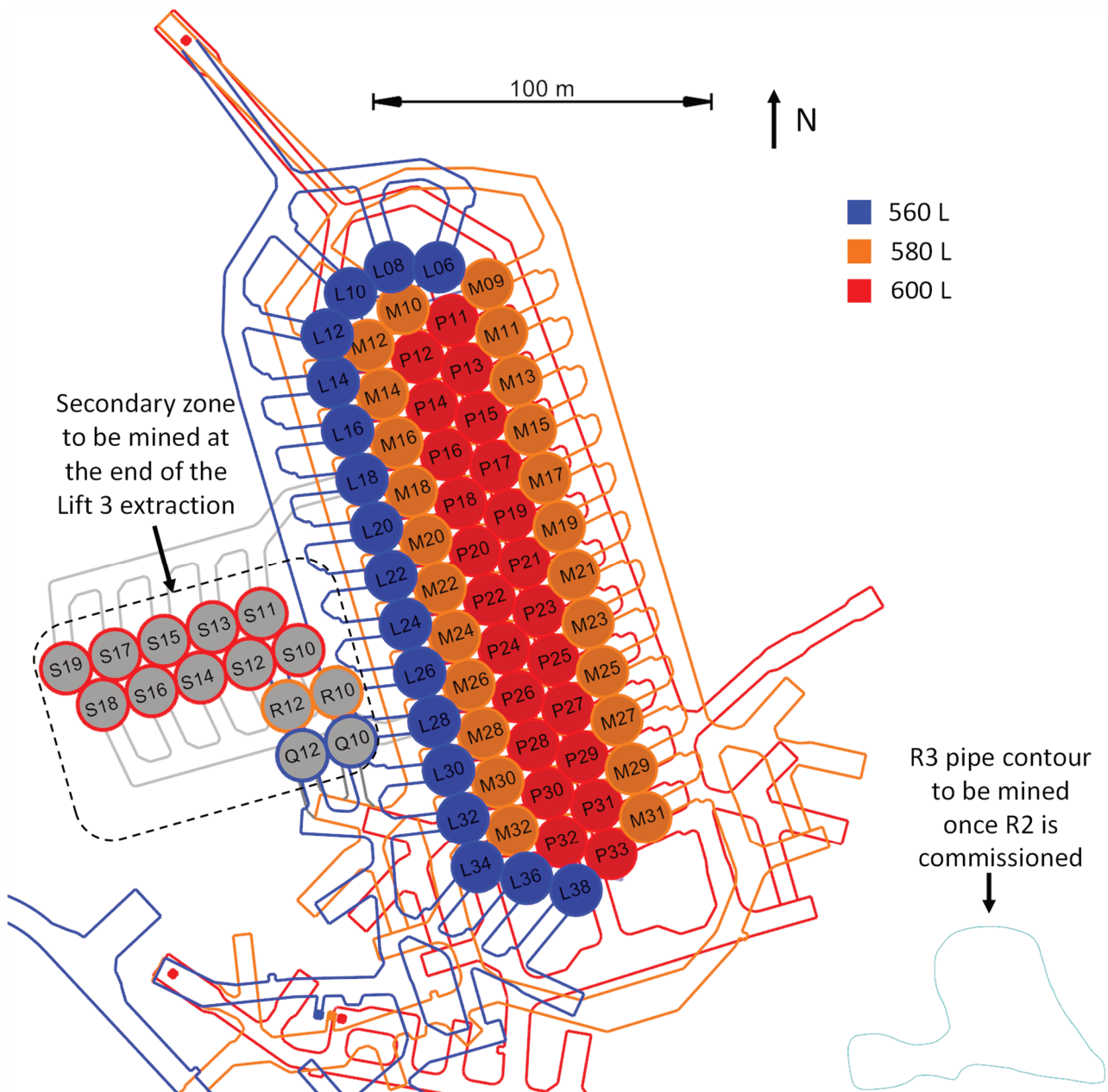

Figure 3   Plan view of the planned R2 Lift 3 levels and draw columns; remnant areas are shaded in grey which will be mined once the primary draw columns are depleted
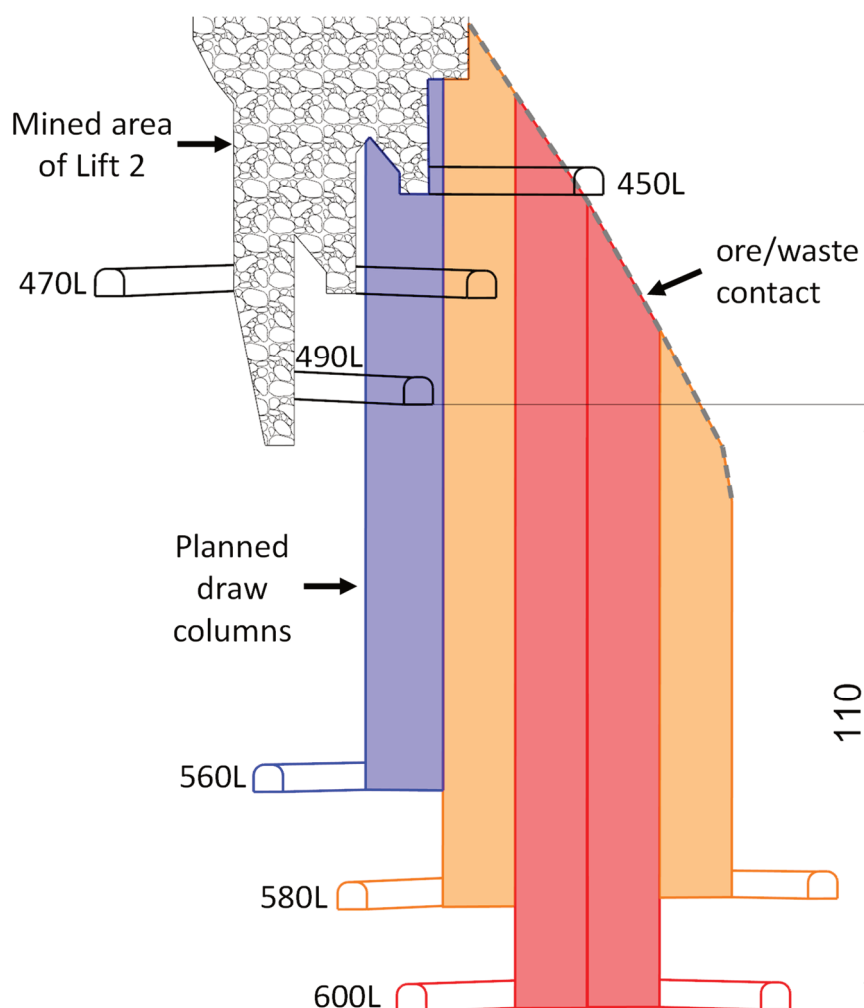
Characterisation of seismic activity at a kimberlite block caving operation in a
complex geological setting in Quebec, Canada

RL Westley-Hauta & S Meyer

Figure 4   Illustrative section view of the planned draw columns and inclined block cave geometry

This mining method was used for Lift 2 extraction during which there were flurries of seismic activity that
motivated the installation of a seismic system in 2021.

1.2   Rock mass properties

Based on analyses following a point load test (PLT) campaign and bonded block model (BBM) simulations,
the following rock mass properties (Table 1) were required in the BBM to achieve a fit for the PLT tests.

Lithology	Rock block strength (MPa)	UCS rm (MPa)	Tensile strength rm (MPa)	Hoek–Brown fits to BBM derived rock mass strength			Young's modulus (GPa)
				m_b	s	a	
KIM2A	28	11.5	0.65	10	0.23	0.61	12.1
KIM2B	36	14.8	0.91	9.5	0.24	0.63	12.1
CR (country rock)	46	18.5	1.31	9.7	0.25	0.65	17.6
CRB (country rock brecchia)	51	20.6	1.17	9.7	0.25	0.65	12.1
Fault/contact	11	4.5	0.28	8.7	0.22	0.6	2.4

Since the variability of the kimberlite rock strength is high, more tests will be completed in the future to quantify this variability. The mine has not completed in situ stress measurements, this topic is addressed in more detail in Section 5.

2 Increase in seismic activity rate and seismic system installation

2.1 Increase in seismic activity rate

The mine had been required to suspend production on March 24, 2020, due to provincially mandated COVID-19 restrictions; the mine had an extended care and maintenance period due to depressed market conditions until operations restarted gradually in September, 2020. The number of 'rock noise incidents' reported by underground workers increased significantly after the full resumption of production activities. Some deformation in the kimberlite was observed to have occurred during the production shutdown, there were no evident signs of seismically induced damage to excavations. While these reports are subjective and affected by numerous factors, the reported increase in 'rock noise' was substantiated by employees who had worked underground long-term at Renard Mine and by underground observations such as sudden damage to excavations, shakedown and projections of rock. A graph showing the cumulative number of 'rock noise incidents' reported by workers and notable events related to the mine's seismicity are shown in Figure 5.
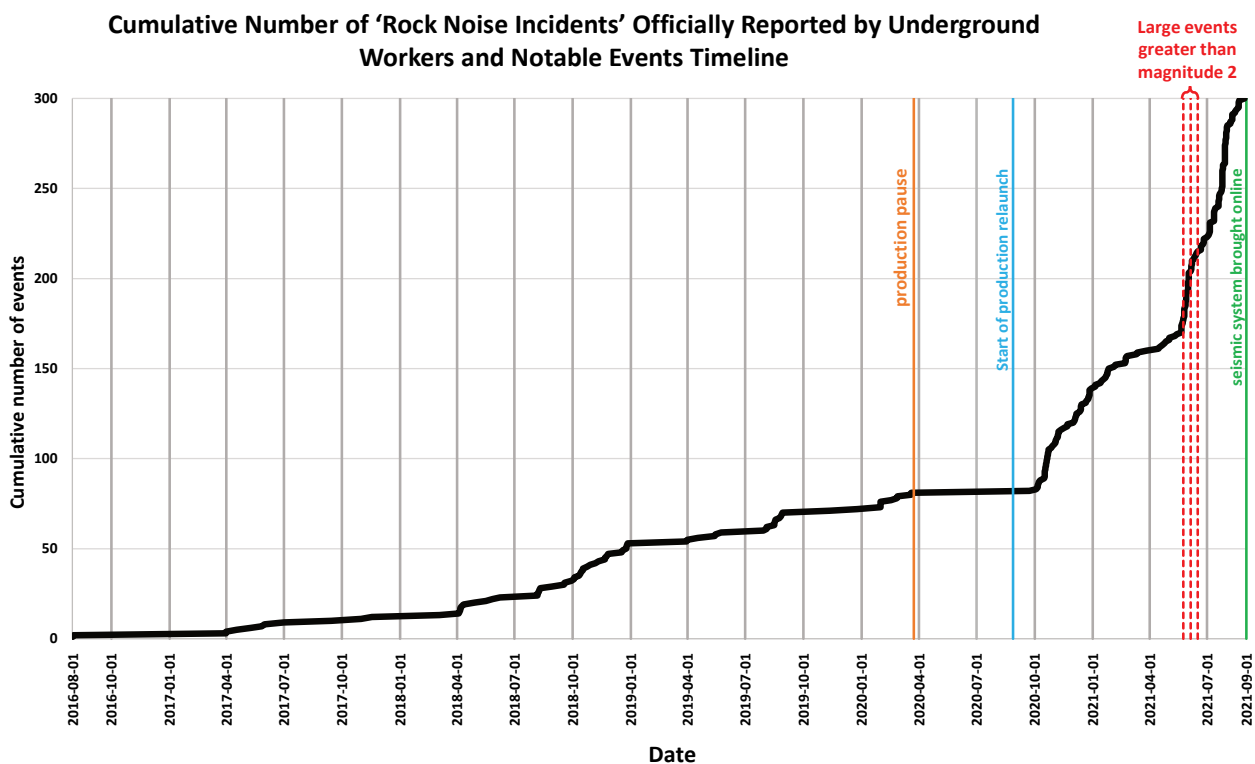

Figure 5   Cumulative number of seismic events reported by underground workers and notable events

The Canadian National Seismograph Network (CNSN) captured three large events during the spring of 2021 (magnitudes are Nuttli magnitude MN):

- May 24, 2021 – MN 2.4.
- June 5, 2021 – MN 2.7.
- June 16, 2021 – MN 2.8.

These events were felt strongly on surface and mine-wide underground. The mine didn't have a seismic system in place at the time; it was presumed by the geotechnical team on site at the start of underground operations that the mine wasn't deep enough to have large seismic events. Once a large event occurred,

Characterisation of seismic activity at a kimberlite block caving operation in a
complex geological setting in Quebec, Canada

RL Westley-Hauta & S Meyer

underground production was temporarily halted, and all accessible drifts were searched by small teams for signs of damage to excavations before resuming production.

Although the mine did not have a seismic monitoring system at the time, the ground motions from some of the events were analysed briefly using a nearby blast vibration monitor on surface. The MN2.4 event on 24 May generated a peak ground motion (PGV) of 2.3 mm/s. The blast vibration monitor contained clear P- and S-wave arrivals from which an approximate hypocentral distance of around 800–1,000 m was estimated using the S-P arrival time separation and some assumed seismic velocities (Meyer 2021). The mine also confirmed that no blasting was done at this time. These observations all lead to the conclusion that this was a significant, genuine seismic event located within the mine.

During this time, there was damage observed to excavations following a series of smaller seismic events in a production area that was traversed by numerous stiff dykes. The mine's capacity to analyse these events beyond spatial and mining factors was limited due to the lack of a seismic system.

2.2 Underground observations and factors associated with three large seismic events

Little damage was observed to active areas following the three large events. After the first large seismic event, a fissure was observed along a fault (NW-01 fault) in an abandoned drilling drift on the 390L which was in proximity to a 90,000 m^3 void in a secondary zone perpendicular to the R2 pipe. The air blast hazard associated with this void had been previously assessed; access to this void was previously blocked with an anti-air blast barricade in the 390L drilling drift. This barricade was constructed with waste rock dans semi-consolidated with shotcrete and designed to withstand pressures associated with the adjacent void. This void was expected to propagate and connect to the Lift 1 zone and fill with waste rock.

During the days following the opening of this fissure along the NW-01 fault, water had begun to seep from the fissure. Following the seismic event on June 5 this fault has slipped approximately 1 m toward the underground void (normal faulting) based on visual observations of the drift displacement. The underground void has been filled with waste rock on June 13 during the connection with Lift 1 as anticipated.

Some additional damage along the fault zone had been observed following the event on June 16, 2021. Photographs of the progression of the slip along this fault are shown in Figure 6.
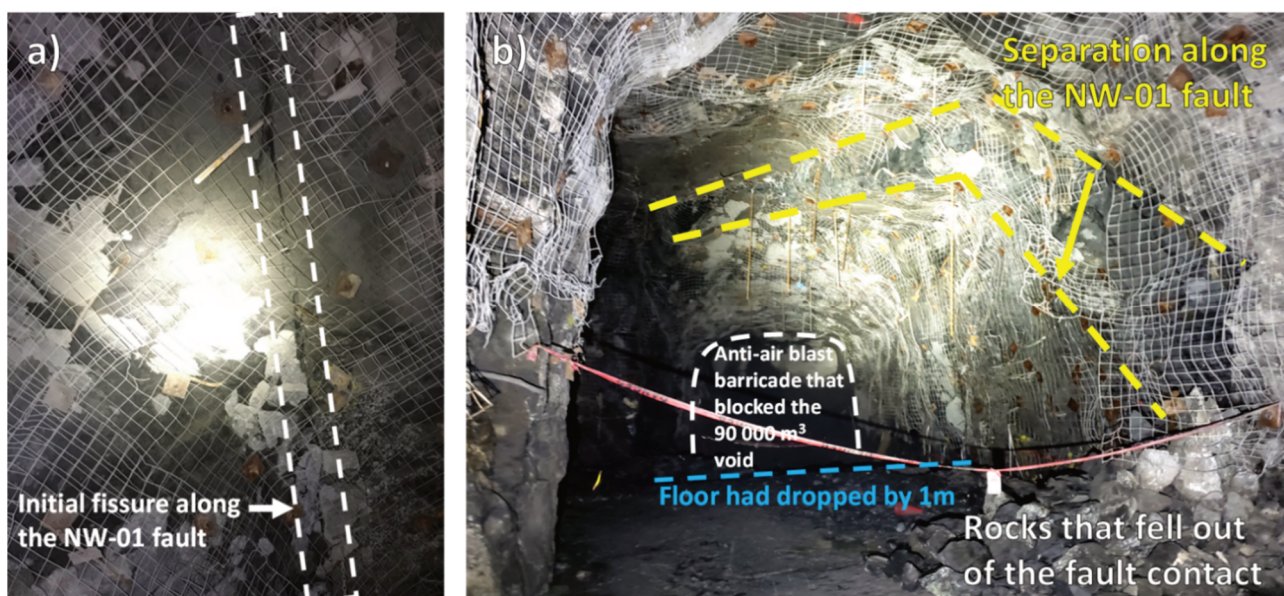

Figure 6 (a) Fissure along the NW-01 fault observed after the event on May 24, 2021; (b) Observed separation along the fault following the two large events in June, 2021

During the time when the large events took place, Renard's management team had decided to accelerate the timeline for the installation of a seismic system.

3 Seismic system installation

3.1 Microseismic equipment

The seismic monitoring system was commissioned in September 2021 in less than one month after receiving the seismic equipment on site. The last 48 hours of seismic activity and blasts are publicly displayed in the operations meeting area.

The system included 27 geophones; 7 triaxial 4.5 Hz, 4 triaxial 14 Hz and 16 uniaxial 14 Hz, standard types of sensors used for seismic monitoring in hard rock mines. The majority of sensors are placed around the R2 pipe with a few in R3. The sensors provide good coverage to the west and south of R2 while the coverage to the east is lacking somewhat, mostly due to the layout of the mine and a lack of locations suitable for sensor installation. The location of events ranges from around 10 m in areas with good coverage to significantly more, on the order of 100 m in areas with poor coverage. The locations of the sensors are shown in Figure 7.
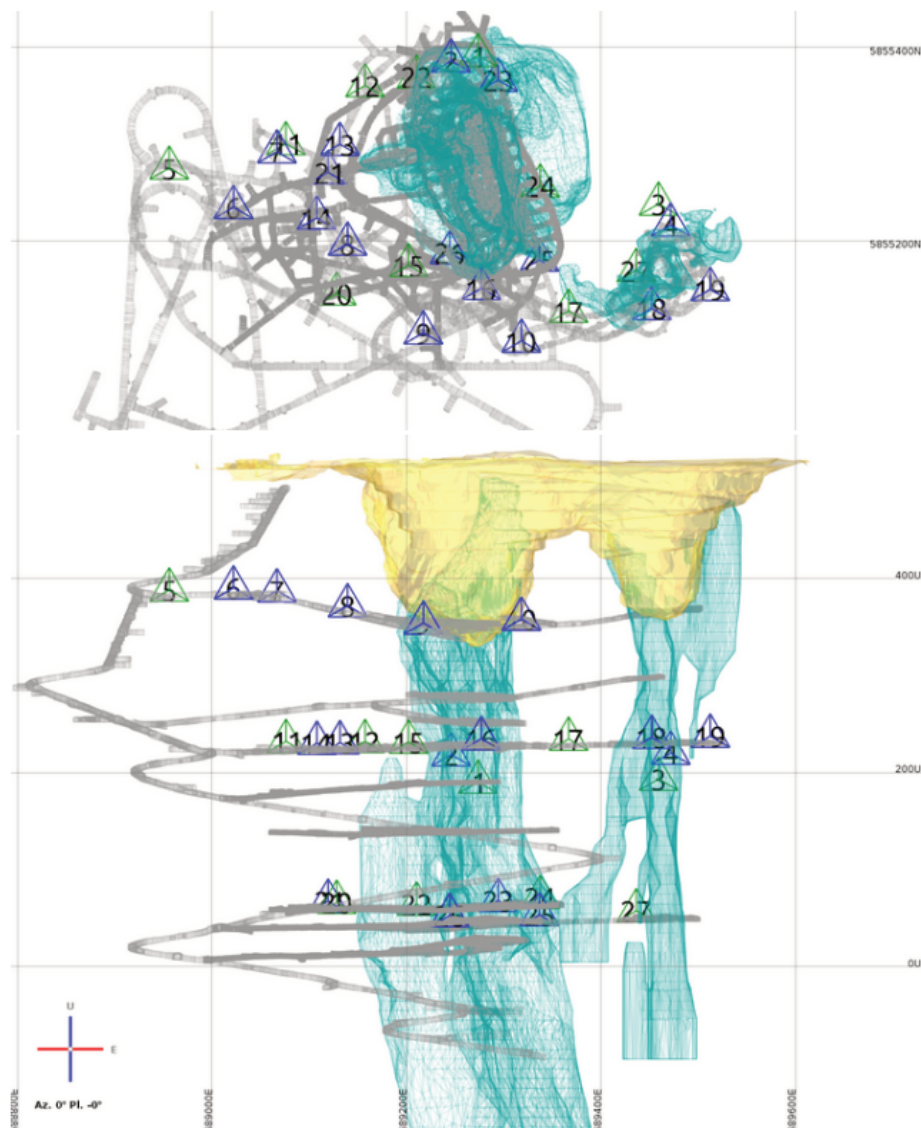

Figure 7   Plan and section views of the installed seismic sensors. Triaxial sensors are shown in green and uniaxial in blue

Characterisation of seismic activity at a kimberlite block caving operation in a
complex geological setting in Quebec, Canada

RL Westley-Hauta & S Meyer

As the mine prepares for Lift 3 in 2022, 8 additional sensors will be installed on the 580 and 600 levels. In addition, seismic instrumentation and monitoring will include the installation of an active seismic source. The aim of this is to investigate if the active source can help identify and track changes in the cave growth. Due to the ductile nature of kimberlite, the caving process is notoriously aseismic, unlike hard rock caving mines, where the cave propagation process generates clear microseismic events ahead of the yield zone that allow the progression of the cave to be monitored fairly easily (Lynch et al. 2018). The use of an active seismic source in underground mines is still fairly experimental, although the methodology has been tested in a few hard rock mines. To our knowledge, this will be the first time it has been attempted in a kimberlite mine.

3.2   Seismic data processing

The system was initially calibrated using 15 calibration blasts situated around the mine, shown in Figure 8.
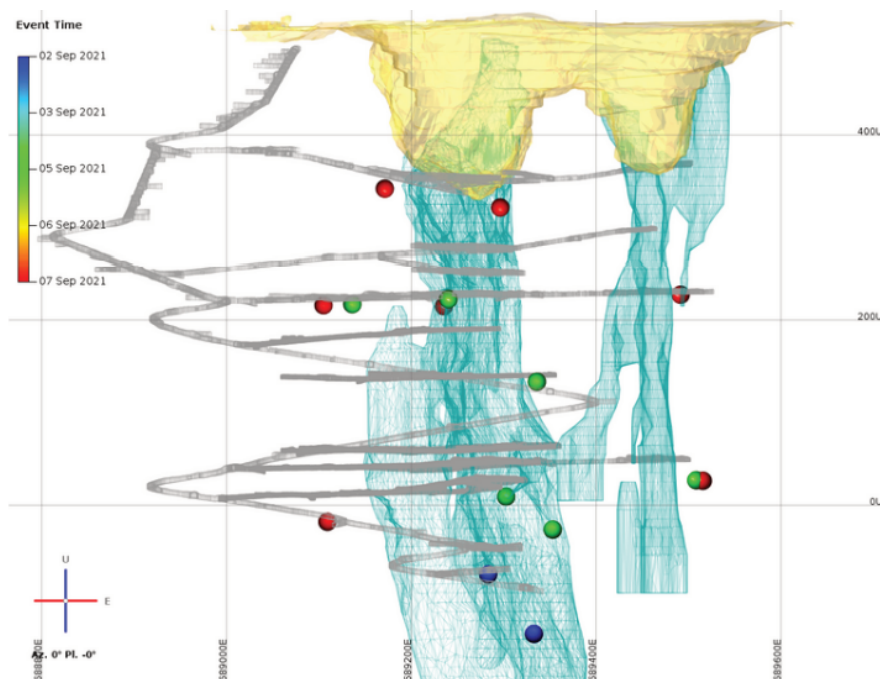

Figure 8   Location of the 15 calibration blasts used to define the velocity model

Due to the presence of the cave and contrasting geological units (kimberlite and host rock), a homogeneous velocity model was not expected to perform well and was not tested. Two velocity model variants, both able to account for velocity heterogeneities were considered; adaptive apparent velocities (Martinsson 2013; Nordström et al. 2017), and a 3D ray tracing mode (Sethian 1996). Adaptive apparent velocities (AAV) performs spatial interpolation of the apparent P- and S-wave velocities between blasts with known locations and the seismic sensors. It is therefore able to capture velocity heterogeneities inherently, such as caves of different geological domains, without explicitly defining them. The 3D ray tracing model however does rely on these different velocity regions to be modelled accurately. While the 3D ray tracing approach may seem more attractive due to being a closer representation of reality, they can be difficult to calibrate and require accurate knowledge of the different velocity regions. As the exact state of the cave is not known, constructing this part of the model is challenging. Furthermore, as the cave is constantly changing, the ray tracing model should be updated constantly which is time consuming. Ultimately, both models were tested. The performance of the models was similar, and AAV was selected for routine processing due to being far simpler to maintain and update than a 3D ray tracing model. Figure 9 compares the performance of the two models on one week worth of data. The overall trends are similar, although the ray tracing model appears to push events on the ends of the monitoring region (far left and far right of figure) slightly further away from the caves.
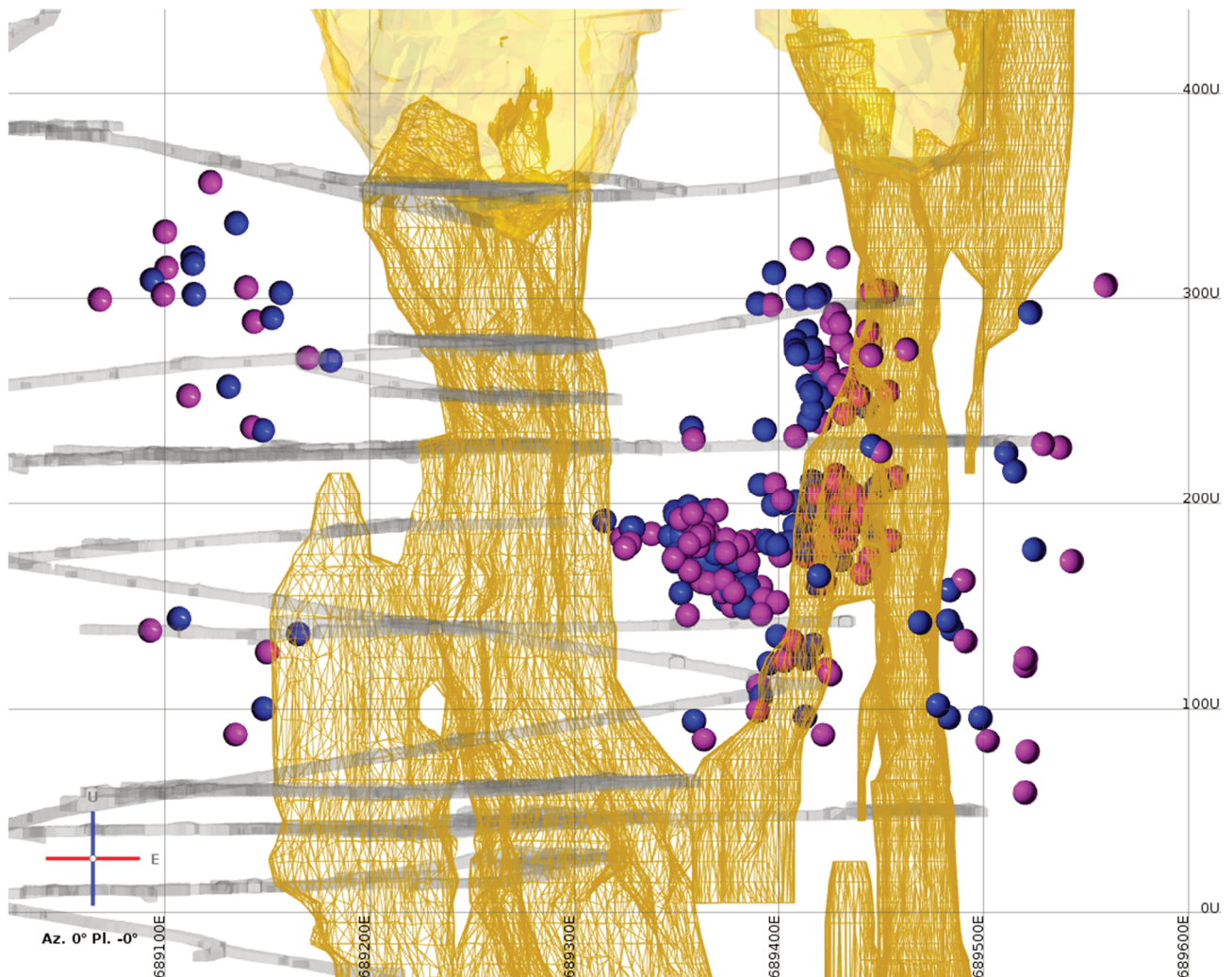
Figure 9 Comparison of event locations according to the ray tracing model (purple) and AAV (blue); qualitatively, the results are similar and the same clusters are trends visible

3.3 Event classification

After routine processing started, it was observed that there were clusters of events appearing in specific working areas such as loading bays. After careful review of the location, timing and waveform characteristics of the events, a few of the clusters were identified as being associated with anthropogenic sources. Three main groups are illustrated in Figure 10. Events associated with a hydraulic hammer that breaks oversize rocks located on surface, were predominantly during the day and had fairly large magnitude, usually between than m_W -0.2 and m_W 0.4 (the mine uses the moment magnitude, m_W, scale). The loading bay group of events showed clear signals, but were often repetitive, had single force mechanisms (rather than moment tensors) and were not present during shift changes and usually had moment magnitudes between m_W -1.0 and m_W 0.0. The final group was located around the extraction level, although complex signals lead to higher location uncertainty and some location scattering. The events were slightly larger in magnitude than the loading bay events and were also absent during shift change/blasting time. These were identified as secondary breaks and strong mechanical impacts from activities on the extraction level.

Characterisation of seismic activity at a kimberlite block caving operation in a
complex geological setting in Quebec, Canada
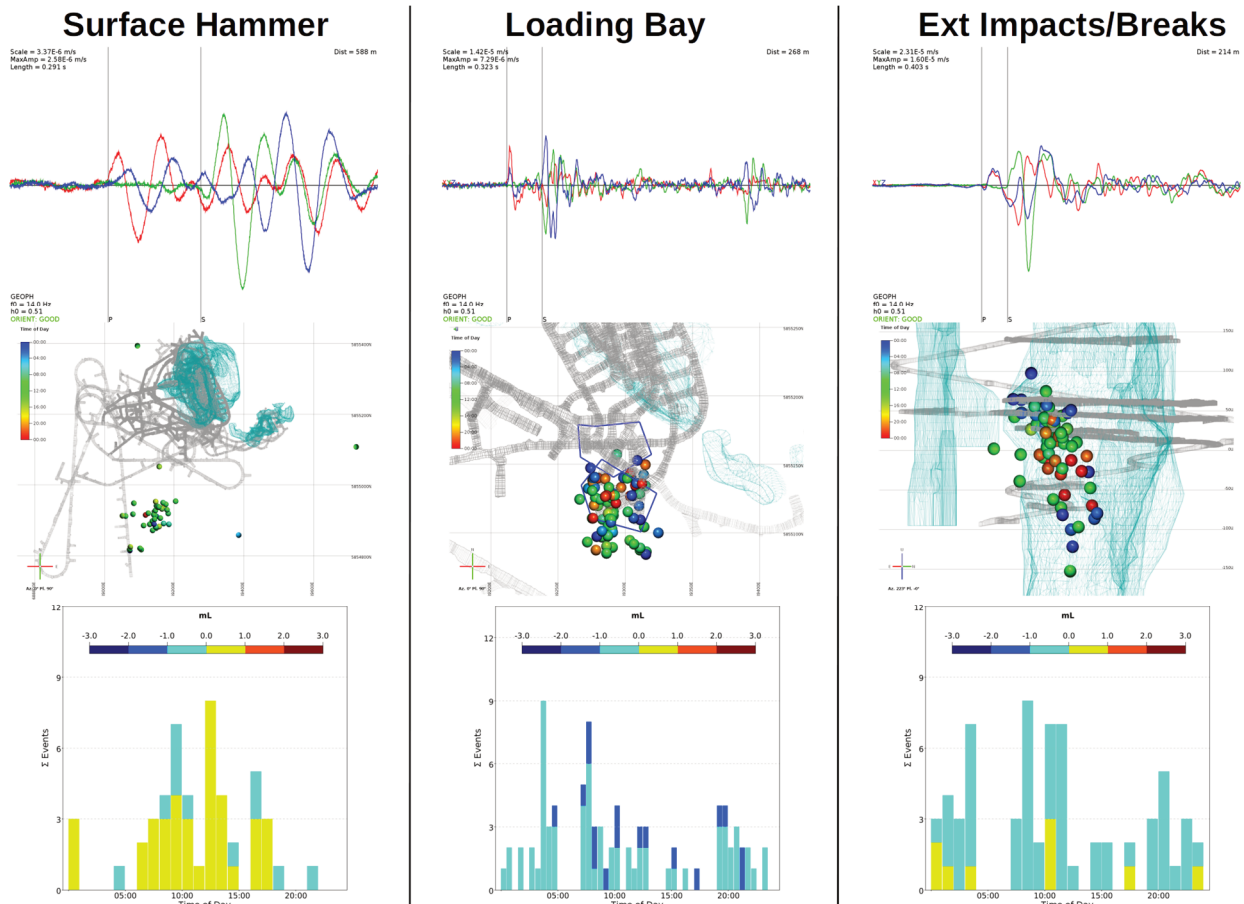
RL Westley-Hauta & S Meyer

Figure 10   Three predominant sources of anthropogenic noise identified in the mine, showing waveforms (top), location (middle) and time of day distribution (bottom)

Such noise sources should be removed from the seismic catalogue, as they do not represent failure of the rock mass in response to mining, and would therefore corrupt any seismological analyses performed. The events are classified as noise in live, routine mode using an event classification scheme based on Malovichko (2012), although some additions and improvements have been made since. Figure 11 provides an example of how the classification system works. A number of features are identified and calculated for calibration events of each event type.
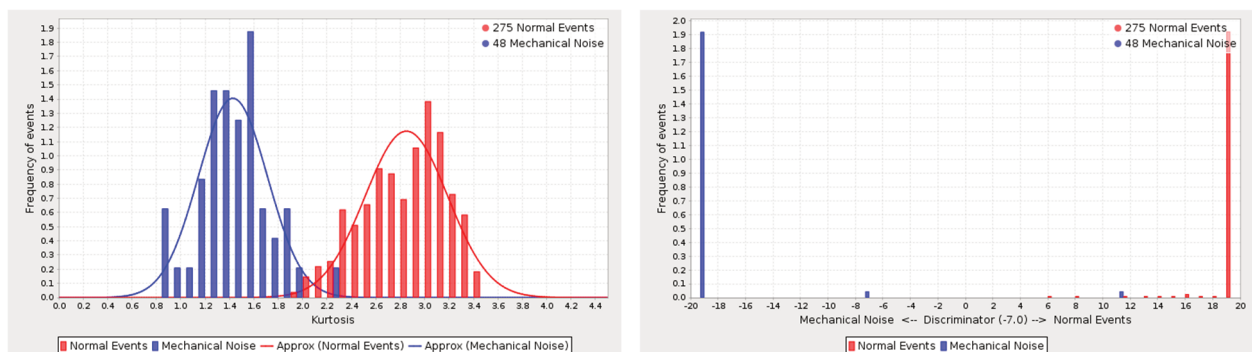

Figure 11   Illustration of the classification method. Example of one feature on the left, and the final discriminating function on the right. One feature is shown as an example, although between 10 and 12 features are used

4.4 Routine source mechanism calculation

Soon after the system was installed, the orientation and response of the sensors were verified. Of the 27 sensors installed, 24 were identified as being suitable for source mechanism inversion. The routine calculation of seismic source mechanisms was then enabled. Of the ~4,100 seismic events recorded to date that have been classified as genuine, seismic source mechanisms have been calculated for ~1,200 of them, or 30%. The majority of the events have predominantly shear type mechanisms, although a few crush type sources are also observed, illustrated in Figure 12.
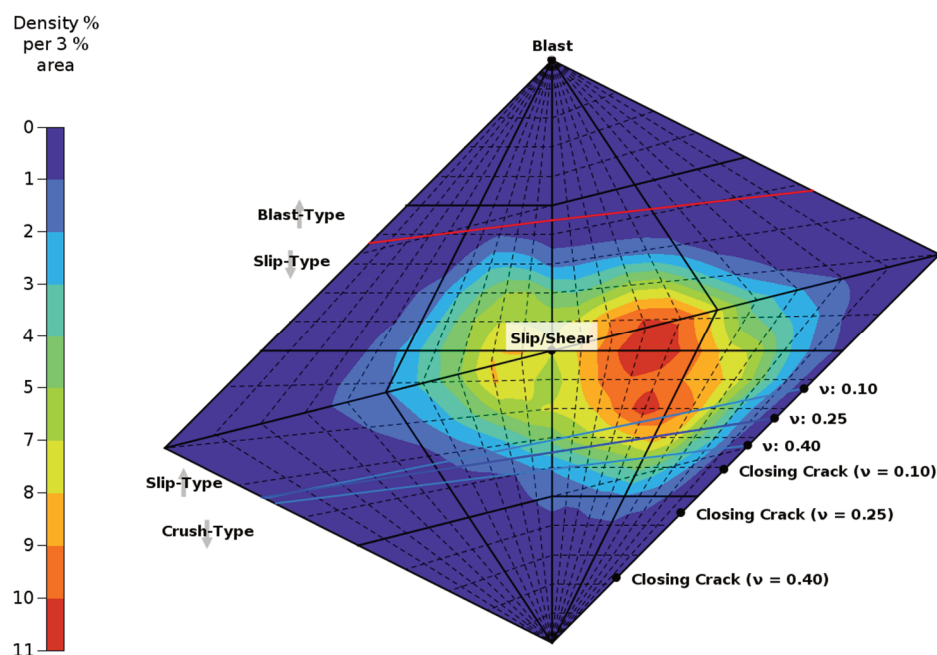

Figure 12 Hudson source-type plot (Hudson et al. 1989) for all seismic source mechanisms recorded to date at Renard Mine

4 Seismic data analysis

4.1 Seismic data overview

The majority of seismic events recorded at Renard locate outside the kimberlite and correspond to slip-type sources. Three main clusters are observed; to the NW of the R2 pipe, between R2 and R3 pipes, and to the SE of R3, shown in Figure 13 by the dashed blue, green, and red circles, respectively. Other, minor clusters of events include low frequency signals around the cave, and crush type sources on development drives. The majority of seismicity, in terms of event numbers and event magnitudes, are located in the central cluster, between the two pipes.
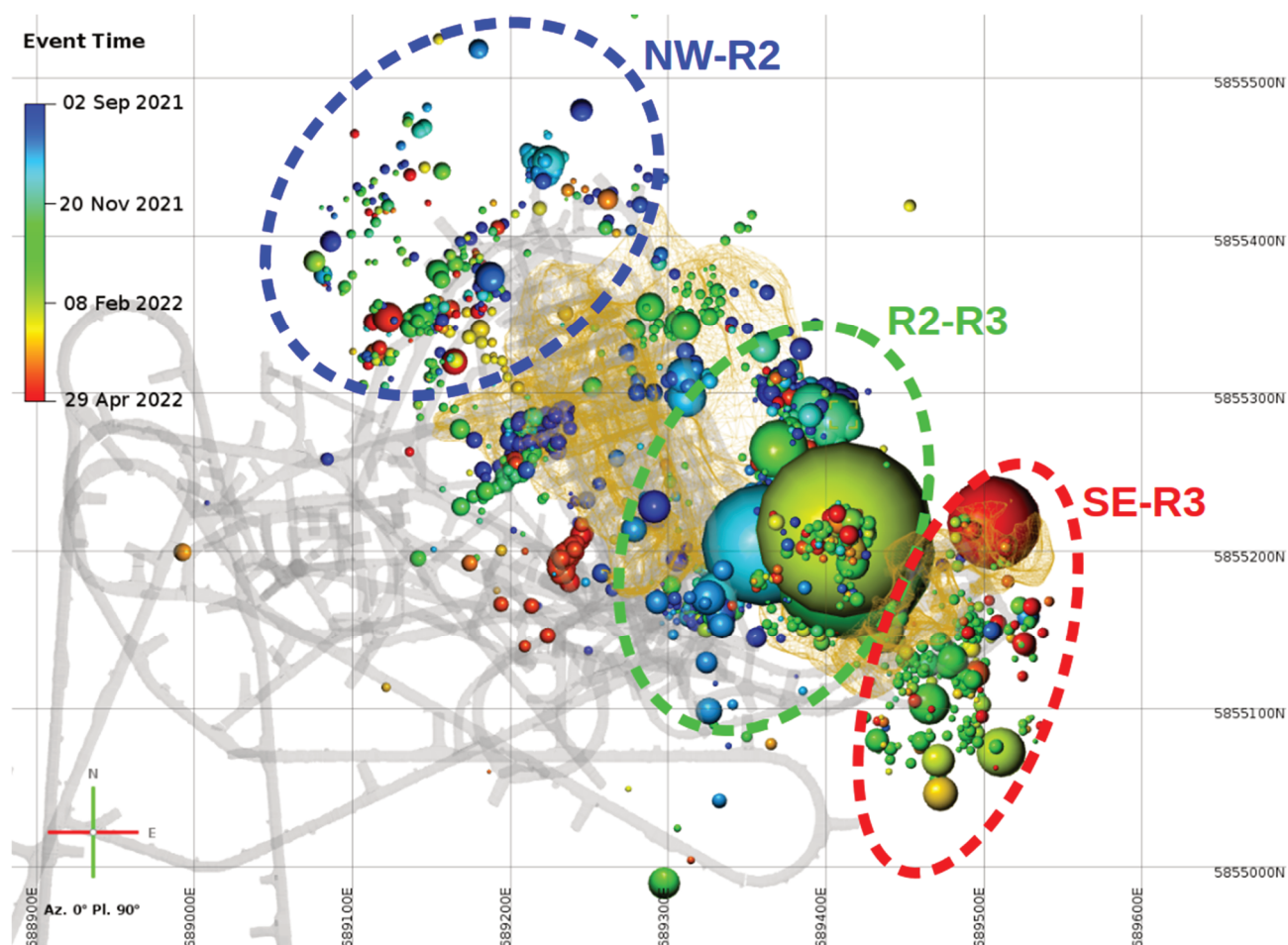
Characterisation of seismic activity at a kimberlite block caving operation in a
complex geological setting in Quebec, Canada

RL Westley-Hauta & S Meyer

Figure 13 Plan view of all events around the mine recorded since the seismic monitoring system was commissioned. Events are coloured to event time and sized according to source radius (assuming an average strain change at source of 10 microstrains for visualisation purposes)

Figure 14 examines the time history of events recorded around the mine, on a mine-wide basis and for the three highlighted regions. The region between the two pipes, R2-R3, has accounted for the majority of recorded events.
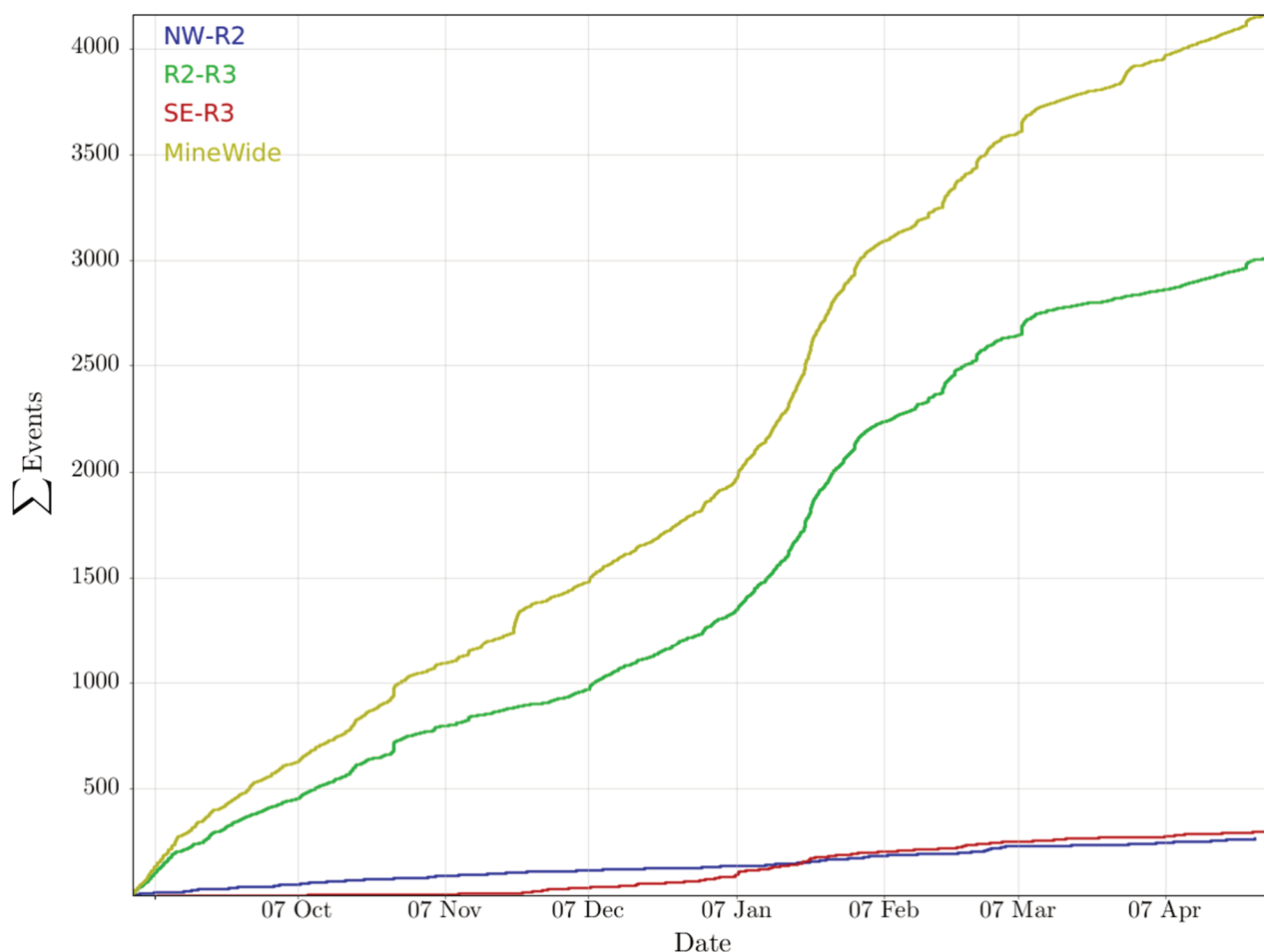
Figure 14 Time history of all events recorded, mine-wide and per region identified in Figure 13

Figure 15 examines the size distribution of events in the different areas and illustrates how the R2-R3 area accounts for the most events as well as the largest events, with the 10 largest events all being in this area. The slope of the distributions vary for different magnitude ranges. If one considers events with $-1.0 \leq m_W \leq -0.3$, the R2-R3 events (green) have the flattest slope while NW-R2 (blue) and SE-R3 (red) have slightly steeper and similar slopes. The number of events in these areas with $mW \geq 0.0$ is fairly low (fewer than 10), which may be related to the relatively short period of monitoring (8 months). It appears as though the NW-R2 and SE-R3 areas have similar behaviour which differs to that of R2-R3. This could be due to the relative positions of these regions, with R2-R3 being between two pipes, while NW-R2 and SE-R3 are at the outer edges of the combined mining area. It is worth noting that the slope of the distributions in each area is roughly the same, indicating that the events are associated with similar source processes.
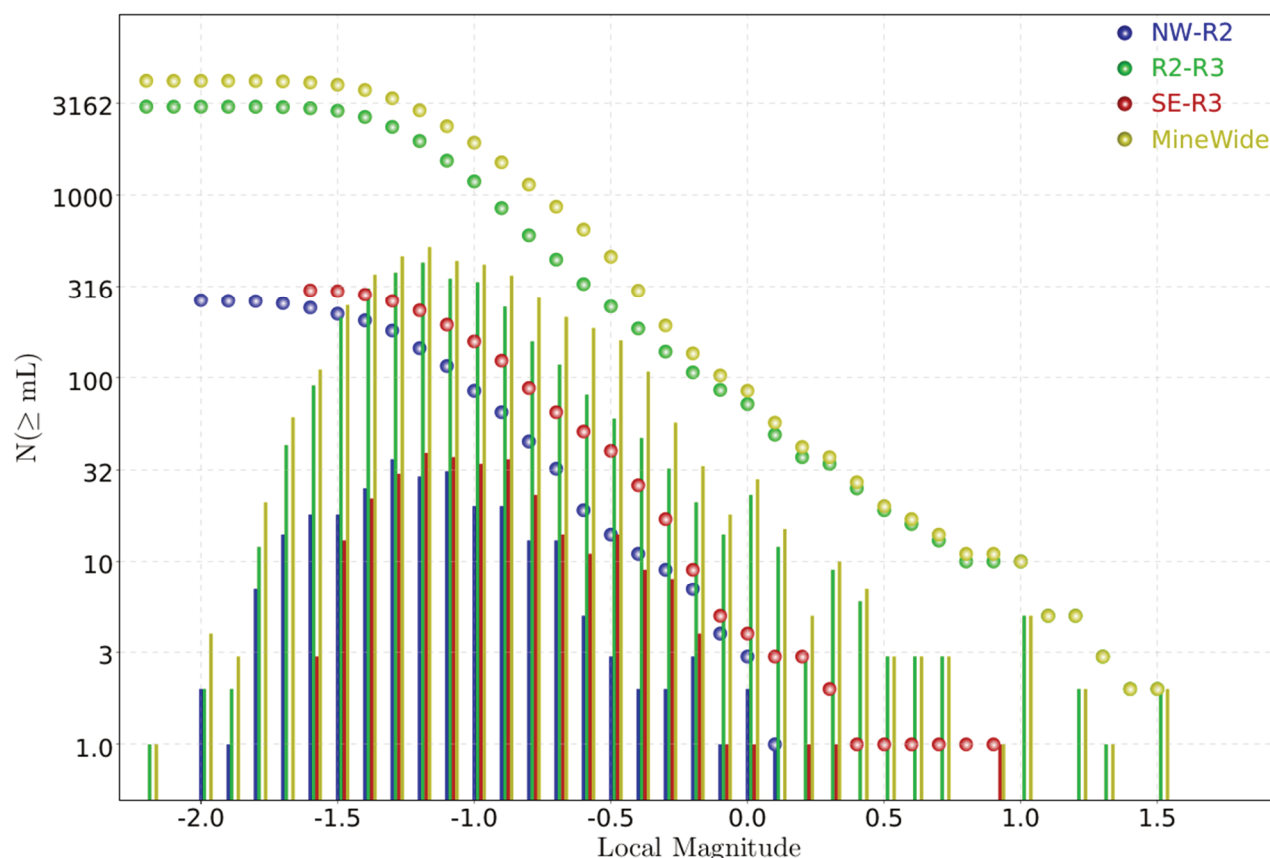
Characterisation of seismic activity at a kimberlite block caving operation in a
complex geological setting in Quebec, Canada

RL Westley-Hauta & S Meyer

Figure 15 Comparative size distribution of the different areas

While the vast majority of the recorded events occur in the host rock surrounding the kimberlite, some seismicity seemingly associated within the pipes is observed. The waveforms are extremely difficult to classify and process. However, a number of events most likely associated with the caving process have been identified. These events were verified as being associated with the caving process based on a combination of location and timing (ruling out the possibility of the signals being associated with machinery). The caving events were found to contain very low frequency waveforms and subsequently had very low energy index, a proxy for the relative energy radiated from a seismic event, regardless of the event size. Figure 16 shows the distribution of events coloured according to Log(energy index) and the Log(energy)-Log(potency) plot used to define the relationship. Note how the caving events, in the centre of the R2 pipe, are those with significantly low Log(energy index) (dark blue).
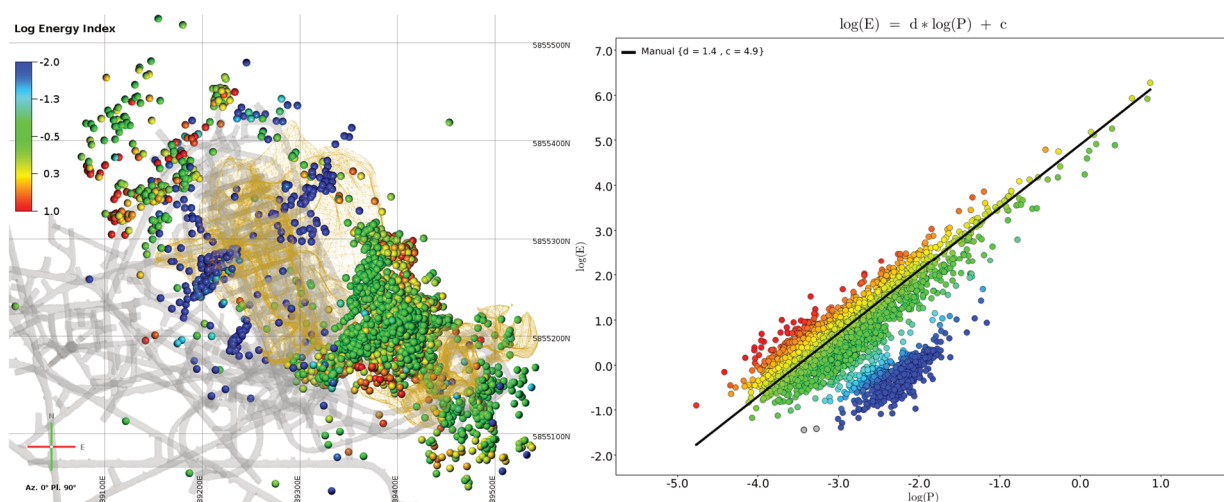
Figure 16 **Plan view of events coloured according to Log (energy index) (left). LogE-LogP plot used to define the energy index relationship**

4.2 Interpretation of data

The majority of recorded events have slip-type sources, as illustrated in Figure 12, and are located in the host rock surrounding the kimberlite pipes. This seismicity is therefore interpreted as shear failure in the host rock due to stress redistribution around and between the kimberlite pipes. Multiple sources appear to be responsible for the shear type events. In some cases, the source mechanisms can be associated to a single, spatially persistent plane which likely indicates a well-defined geological structure, such as a fault, dyke or lithological contact. In other cases, the source mechanisms of the events are more scattered and no clear, well-defined planar feature matching both locations and nodal planes can be identified. In such cases, the failures can likely be attributed to minor weaknesses such as small joints or fractures with scattered orientations. Figure 17 illustrates the identification of the former case, an existing and spatially persistent plane of weakness, located to the SE of the R3 pipe. The structure is verified through the consistent source mechanisms, where the one nodal plane solution is parallel to the spatial distribution of event locations. The events associated are reverse faulting with the orientation of the best approximated plane being dip = 30°, dip direction = 230°.
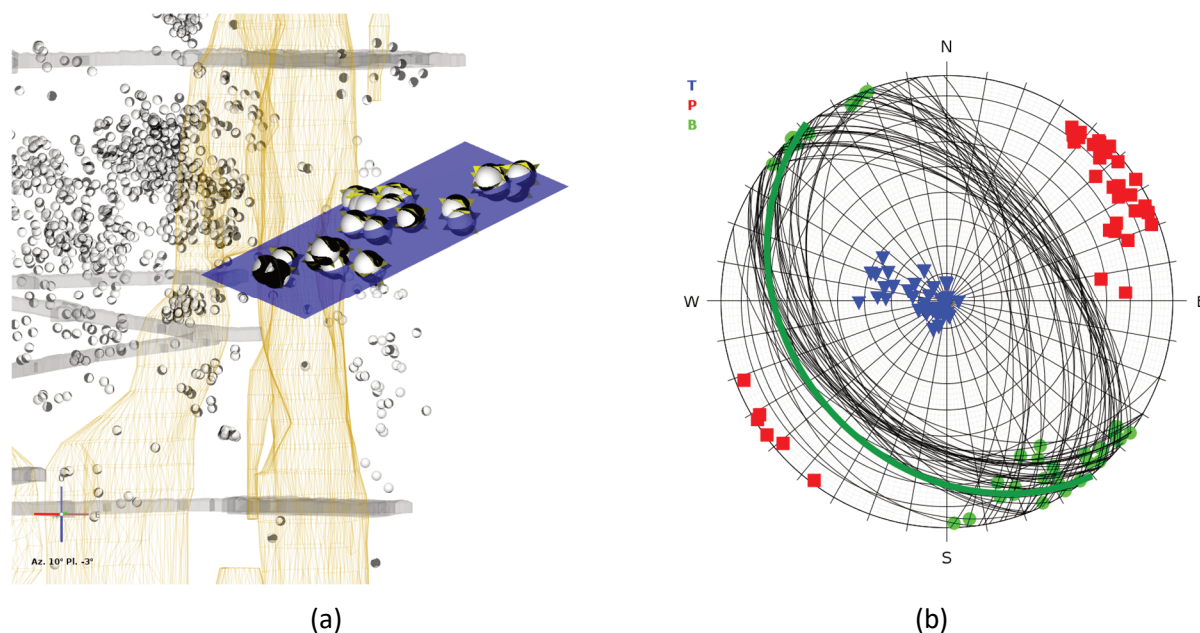

(a)   (b)

Figure 17 **Example of an identified, seismically active, weak planar feature. (a) Beachballs and approximated plane; (b) Stereonet**

Characterisation of seismic activity at a kimberlite block caving operation in a
complex geological setting in Quebec, Canada

RL Westley-Hauta & S Meyer

5   In situ stress measurements and numerical model calibration

No in situ stress measurements have been conducted at Renard Mine. The in situ stress tensor was presumed to be horizontal at 55 degrees by the mine's rock mechanics consultants using the world stress map from 2010 (Figure 18 and Table 1) and typical values for the Canadian shield which was deemed sufficient at the time for shallow open pit designs. This stress direction was assumed for the numerical models for underground workings at depth as late as 2020 (Bouzeran et al. 2020).
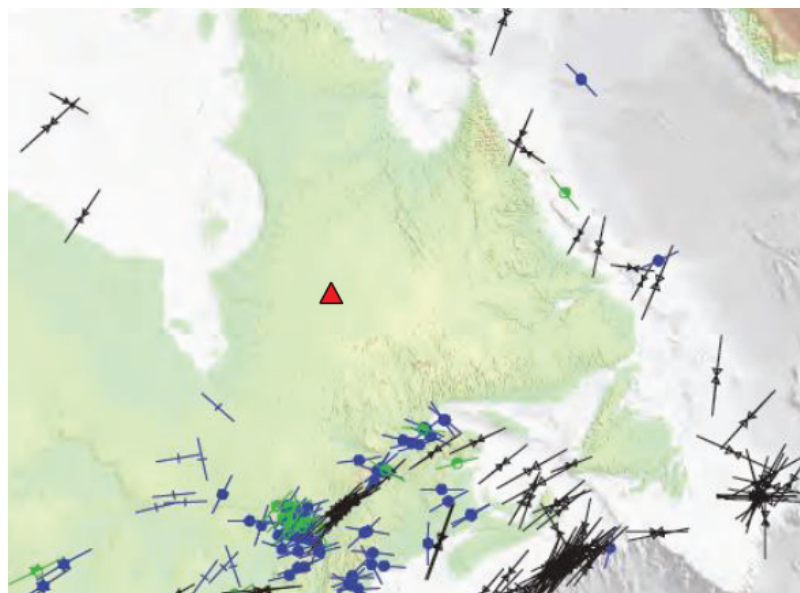

Figure 18 World stress map (from Heidbach et al. 2008) that was used to presume the in situ stress orientation (Brummer 2010); note the lack of data points in proximity to the mine site (red triangle) and the variability in the stress orientations surrounding the site

Table 1   Presumed in situ stress environment (Brummer 2010; Bouzeran et al. 2020)

Principal stress	Magnitude	Trend	Plunge
Major	$1.8*\sigma_3$	N55E	0
Medium	$1.4*\sigma_3$	N145E	0
Minor	$\rho*g*h$	–	90

The observed deformation in drifts and direction of squeezing/shifting in boreholes was not in the expected orientation using this assumed in situ stress environment.

The orientation of the combined regional and induced stress field was investigated by comparing moment tensor decompositions to numerical modelling results. Map3D numerical stress models (Wiles 2010) were run for different orientations of principal stresses, with horizontal σ_1 varying from 0 to 80 degrees, in 5 degree increments on a 20 m evenly spaced grid for two different time periods:

- Time period 1 (t1) where the connection between Renard 3 Lift 1 and Renard 3 Lift 2 had not taken place.

- Time period 2 (t2) after the connection had taken place.

It was presumed that this connection will affect the P-axes of the moment tensor results, specifically for the events located between the R2 and R3, and surrounding the R3 pipe. The details of the comparison process are described below:

1. Run elastic Map3D numerical stress models for different orientations of principal stresses, with horizontal σ_1 varying from 0 to 80 degrees, in 5 degree increments.

2. Seismic data from the two time periods were used to calculate the coseismic strain field. This methodology evaluates characteristics of rock mass deformation based on an aggregate of the recorded seismic events and is described in detail in Malovichko (2022).

3. The coseismic strain field is evaluated on a regular grid. At each grid point, the direction of the averaged P-axes from seismic source mechanisms (proxy of local σ_1) is compared to the modelled σ_1 at the same location. The angular difference between the observed P-axes and modelled σ_1 is calculated at each grid point, for each model.

4. The average difference for each model, across all grid points, is calculated to provide some measure of the agreement between observed data and the numerical stress model.

Another potential approach would have been to apply direct stress inversion methods (Michael 1984; Hardebeck & Hauksson 2001), as are commonly used in crustal seismology. While this seems appealing due to the well-established and proven methodology, the methods are not always applicable in a mining environment. From Hardebeck & Hauksson (2001), two fundamental assumptions that need to be met for stress inversion to be applied:

- All methods for inverting focal mechanisms for stress orientation rest on the assumption that earthquakes slip in the direction of the resolved shear stress on the fault plane.

- The four stress parameters are constant over the spatial and temporal extent of the dataset.

The first of these essentially states that slip-type mechanisms are required. Usually, in mines, this may not always be the case, as the presence of the man-made excavations leads to "crush" type sources being very common. In our case, we are specifically filtering on slip events, so this first assumption is met. The reason why typical stress inversion methods are not appropriate in our case is the 2nd assumption above, that the stress state is constant in time and space. Due to the presence of the caved region and close proximity of the events to it, the stress field is most definitely not constant in space and is exactly why numerical modelling is integrated into the method.

The above-described process is illustrated in Figure 19. For each grid point, the orientation of the maximum principal coseismic strain direction is compared to the direction of modelled σ_1. Comparing 0 degrees (left) and 55 degrees (right) models shows that in the R2-R3 interaction area, the 0 degree model generally results in very low angular misfits, with a large number of blue spheres. For the 55 degree model, this area shows much higher misfits, with green and orange spheres visible. Some areas, such as to the SE of R3 show lower misfit for the 55 degree variant though.
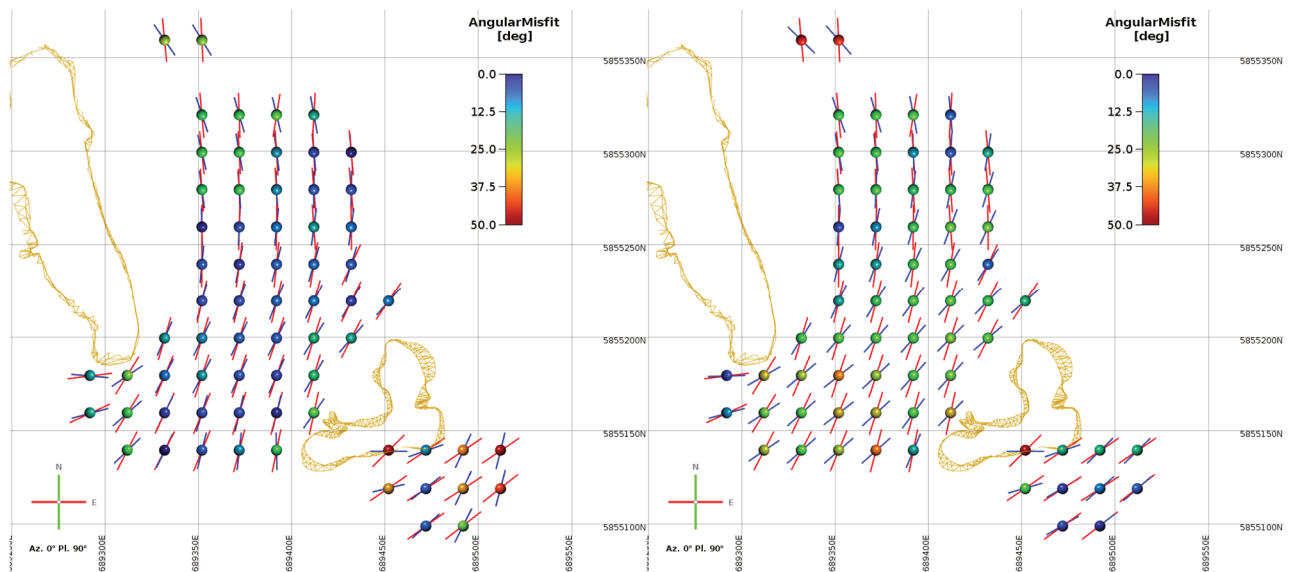
Characterisation of seismic activity at a kimberlite block caving operation in a
complex geological setting in Quebec, Canada

RL Westley-Hauta & S Meyer

Figure 19 Illustration of the stress direction verification. Horizontal slices around Z = 155–175. Red vectors indicate the direction of maximum compressive strain inferred from seismic data. Blue vectors indicate the modelled direction of σ_1 for in situ σ_1 = 0 degrees (left) and 55 degrees (right). The spheres are coloured according to the angular misfit between the two angles

Figure 20 plots the average misfit across all grid points for the two time periods. Time Period 1 had the lowest misfits around 0–5 degrees while for period 2, the lowest misfits were found for 15–30 degrees. Experience and observations at the mine (e.g. borehole dislocation) lead to σ_1 having an expected range of also around 15–30 degrees. While the two time periods do not agree entirely, they are similar, are significantly different from the 55 degrees which had been assumed by rock mechanics consultants in the earlier days of mining.
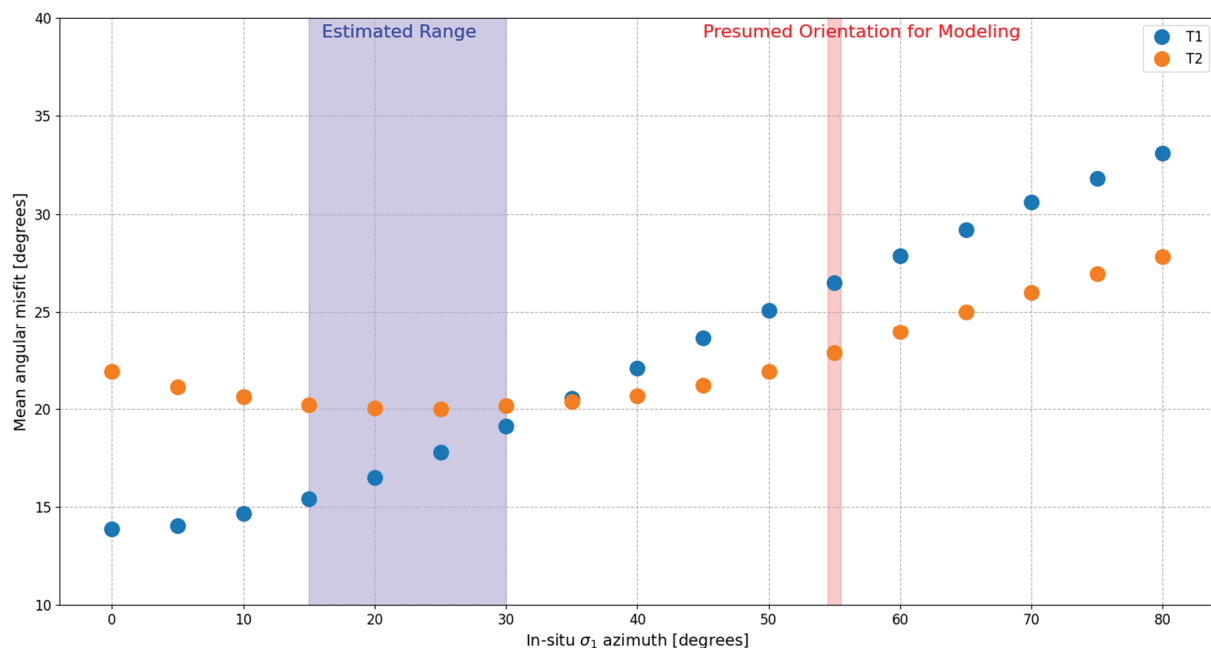

Figure 20 Average angular difference between estimated σ_1 direction from seismic data and modelling for the two time periods

Although the results from the two periods did not agree exactly, they were similar enough to indicate that the in situ σ_1 should be closer to N-S than originally presumed. There are a variety of reasons that could explain the mismatch, from the seismological and numerical modelling sides. Some of the more likely reasons include:

- For the maximum coseismic strain direction to match the maximum principal stress direction, the slip sources need to occur on a collection of weakness with varying orientation. If a large portion of the events are associated with a single, persistent structure or feature, then the orientation of that feature dictates the orientation of the seismic P-axes and subsequent strain direction (this assumption is also applicable to stress inversion techniques). Figure 17 indicates that this factor is playing at least some role.

- Numerical modelling was assumed to be elastic. It is possible that the yielding behaviour of the rock mass needs to be accounted for to properly estimate the orientation of the stress field.

- Uncertainty in seismic data. Due to the presence of the caves, the coverage of events for purposes of seismic source mechanism inversion is not perfect. Furthermore, interaction of the seismic waves with the caves introduces complexity to the waveforms which can impact the source mechanism inversion and even event location estimation.

These results are considered preliminary and show promise at using the microseismic data to verify the assumptions of the stress field at the mine. The work is ongoing, and future plans are discussed in the following section.

6   Discussion and future work

Using eight months of seismic data, important insights into the nature of Renard Mine's seismicity and rock mass response to mining have been observed, mainly:

- The majority of seismic events take place outside of the mine's main workings which supports observations made (such as borehole shift direction, deformation orientations in drifts) prior to the seismic system installation.

- Major structures are seismically active and contribute to the mine's seismicity; this improves the mine's understanding of the contribution of structures to seismicity.

- Seismic activity takes places in distinct zones which are associated with distinct seismic behaviour.

- The in situ stress field is in a more north–south orientation, potentially around 30 degrees, than the initially presumed 55 degrees. The new input parameters provide improved model results. These results can be tested using the orientation of the seismic source mechanisms.

Although the initial comparison of seismic data with numerical modelling shows some promise, it was a first attempt, and the work is ongoing. In the next iteration of analysis, instead of averaging the seismic source mechanisms to estimate the orientation of the coseismic strain field, we plan on focusing on the stresses at the event locations instead. A simple approach is to compare the P-axes with the orientation of σ_1. This may give some idea, but as mentioned previously, for existing weaknesses, the orientation of the source mechanism is controlled by the orientation of the weakness, and not the exact orientation of σ_1 (or the P-axes, the geological structure just has to be favourable for slip). Rather, we plan on calculating the modelled direction of shear traction on each nodal plane and comparing this to the observed direction of slip, as this should provide a more direction comparison of the relationship between stress directions and event orientations.

During 2022 and early in 2023, the undercut in Renard 2 Lift 3 will be excavated, and the connection between R2L3 and R2L2 will be made. The recorded seismicity during this phase of mining will be important to understand the stress redistribution for an entire mining zone, and to complete forward projections for future mining zones. The active source will be used along with seismic data to attempt to estimate the evolution of the R2L3 cave growth.

Characterisation of seismic activity at a kimberlite block caving operation in a
complex geological setting in Quebec, Canada

RL Westley-Hauta & S Meyer

7 Conclusion

Following a series of large seismic events at Renard Mine, a seismic system was installed to quantify the seismic activity in the underground mine workings and to provide insight into the rock mass response to mining.

The preliminary results using only months of data have allowed the mine to identify the seismically active regions and potential sources of large events, improve the understanding of the in situ stress tensor which allows the mine to run improved numerical models to estimate the effects of mining on the underground workings.

As the mine expands, new seismic sensors will be installed to maintain an adequate system sensitivity in all active zones. An active source will be installed before the start of undercut blasting in Renard 2 Lift 3, and an attempt will be made to track that zone's cave growth with improved accuracy.

The seismic system installation and preliminary results analysis was a success, and it provides the operation with insight into the rock mass response to mining and peace of mind by understanding the nature of the mine's seismicity.

Acknowledgement

References

Bouzeran, L, Fuenzalida, M & Pierce, M 2020, *Advanced Caving Analysis for Renard Mine — R2 Pipe Lift 2*, internal report.

Brummer, RK 2010, *Mine Design Interim Report – Stornoway - In-situ Stress*, internal report.

Hardebeck, JL & Hauksson, E 2001, 'Stress orientations obtained from earthquake focal mechanisms: What are appropriate uncertainty estimates?', *Bulletin of the Seismological Society of America*, vol. 91, no. 2, pp. 250–262.

Heidbach, O, Tingay, M, Barth, A, Reinecker, J, Kurfeß, D & Müller, B 2008, *The World Stress Map Database Release 2008*, Deutsches GeoForschungsZentrum GFZ, Potsdam, https://doi.org/10.1594/GFZ.WSM.Rel2008

Hudson, JA, Pearce, RG & Rogers, RM 1989, 'Source type plot for inversion of the moment tensor', *Journal of Geophysical Research*, vol. 94, no. B1, pp. 765–774.

Lépine, I & Farrow, D 2018, '3D geological modelling of the Renard 2 kimberlite pipe, Québec, Canada: from exploration to extraction', *Mineralogy and Petrology*, vol. 112, no. 2, pp. 411–419.

Lynch, R, Meyer, S, Lotter, E & Lett, J 2018, 'Tracking cave shape development with microseismic data', in Y Potvin & J Jakubec (eds), *Caving 2018: Proceedings of the Fourth International Symposium on Block and Sublevel Caving*, Australian Centre for Geomechanics, Perth, pp. 555-564, https://doi.org/10.36487/ACG_rep/1815_43_Lynch

Malovichko, D 2012, 'Discrimination of blasts in mine seismology', in Y Potvin (ed.), *Deep Mining 2012: Proceedings of the Sixth International Seminar on Deep and High Stress Mining*, Australian Centre for Geomechanics, Perth, pp. 161–172, https://doi.org/10.36487/ACG_rep/1201_11_malovichko

Malovichko, D 2022, 'Utility of seismic source mechanisms in mining', *Proceedings of the Tenth International Symposium on Rockbursts and Seismicity in Mines*, Society for Mining, Metallurgy & Exploration, Englewood.

Martinsson, J 2013, 'Robust bayesian hypocentre and uncertainty region estimation: The effect of heavy-tailed distributions and prior information in cases with poor, inconsistent and insufficient arrival times', *Geophysical Journal International*, vol. 192, no. 3, pp. 1156–1178, https://doi.org/10.1093/gji/ggs067

Michael, J 1984, 'Determination of stress from slip data: Faults and folds', *Journal of Geophysical Research: Solid Earth*, vol. 89, pp. 517–526.

Meyer, S 2021, *Renard Mine: Preliminary Observations from Blast Vibration Monitoring*, technical report, Institute of Mine Seismology, Kingston.

Nordström, E, Dineva, S & Nordlund, E 2017, 'Source parameters of seismic events potentially associated with damage in block 33/34 of the Kiirunavaara mine (Sweden)', *Acta Geophysica*, vol. 65, no. 6, pp. 1229–1242, https://doi.org/10.1007/s11600-017-0066-1

Sethian, JA 1996, 'A fast marching level set method for monotonically advancing fronts', *Proceedings of the National Academy of Sciences*, vol. 93, no. 4, pp. 1591–1595

Wiles, TD 2010, *Map3D*, computer software, Map3D International Ltd, www.map3d.com